OPEN ACCESS

Cancer Clinical Trials ARTICLE

The Innovation Oncology

Exhaled volatile organic compounds as predictors of chemoradiotherapy response in locally advanced ESCC: A prospective study

Yilu Gao,[1,2,4] Xingyuan Cheng,[1,2,4] Baoqing Chen,[1,2,3,4] Lei Zhao,[1,2] Shiliang Liu,[1,2] Yingxin Lv,[1,2] Qiaoqiao Li,[1,2,*] Yujia Zhu,[1,2,*] and Mian Xi[1,2,3,*]

*Correspondence: ximian@sysucc.org.cn (M.X.); zhuyuj@sysucc.org.cn (Y.Z.); liqq@sysucc.org.cn (Q.L.)

Received: June 3, 2026; Accepted: August 26, 2026; Published Online: September 10, 2026; https://doi.org/10.59717/j.xinn-oncol.2026.100040

GRAPHICAL ABSTRACT

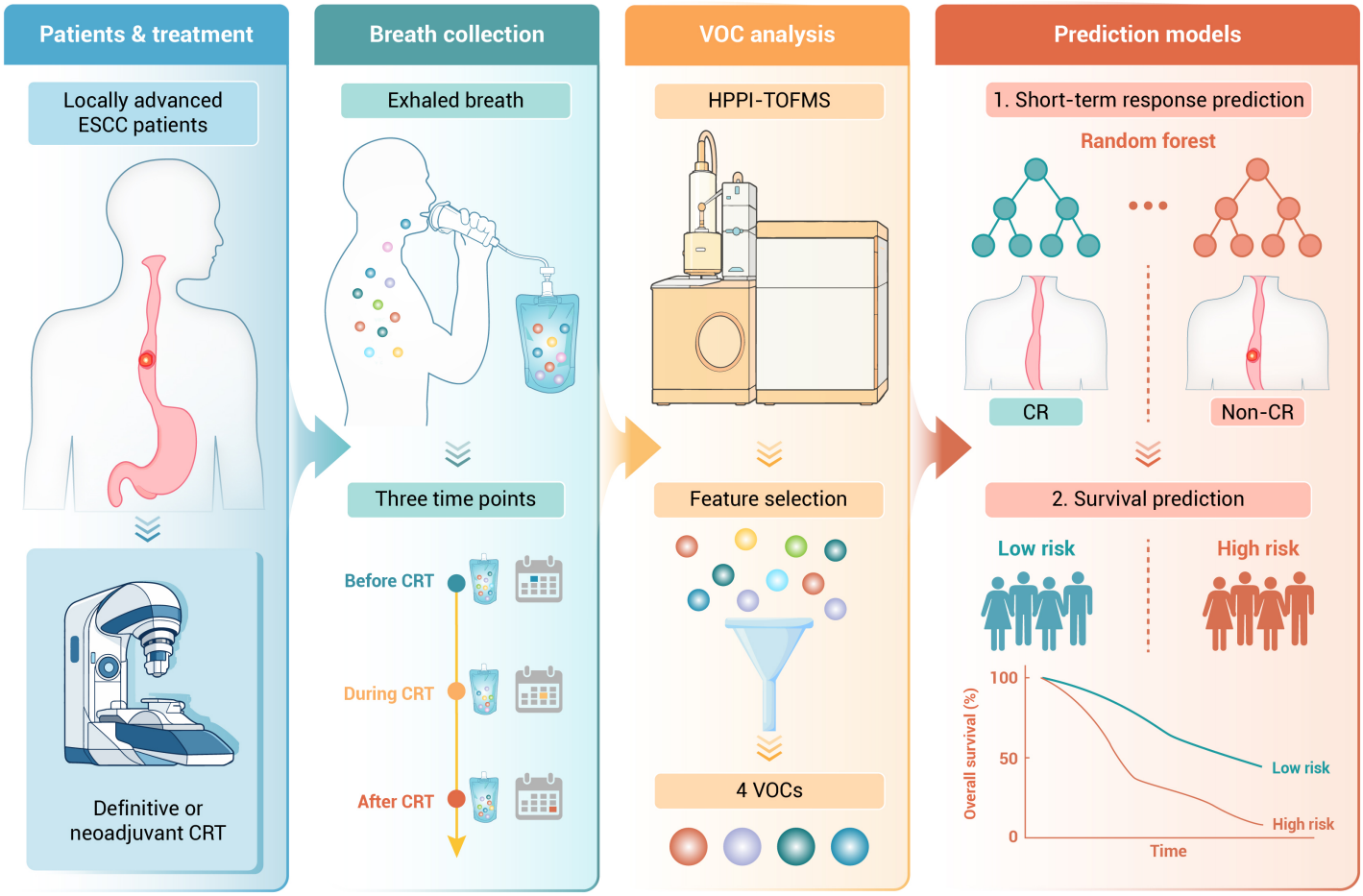

PUBLIC SUMMARY

- Volatile organic compounds (VOCs) predict outcomes in esophageal squamous cell carcinoma (ESCC).
- VOCs dynamically change during chemoradiotherapy (CRT) and vary between complete response (CR) and non-CR.
- Breath-based biomarkers may help monitor ESCC in real time and guide personalized therapy.

ARTICLE Cancer Clinical Trials

Exhaled volatile organic compounds as predictors of chemoradiotherapy response in locally advanced ESCC: A prospective study

Yilu Gao,[1,2,4] Xingyuan Cheng,[1,2,4] Baoqing Chen,[1,2,3,4] Lei Zhao,[1,2] Shiliang Liu,[1,2] Yingxin Lv,[1,2] Qiaoqiao Li,[1,2,*] Yujia Zhu,[1,2,*] and Mian Xi[1,2,3,*]

[1]State Key Laboratory of Oncology in South China, Collaborative Innovation Centre for Cancer Medicine, Guangdong Esophageal Cancer Institute, Guangzhou 510060, China

[2]Department of Radiation Oncology, Sun Yat-sen University Cancer Center, Guangzhou 510060, China

[3]United Laboratory of Frontier Radiotherapy Technology of Sun Yat-sen University & Chinese Academy of Sciences Ion Medical Technology Co., Ltd, Guangzhou 510060, China

[4]These authors contributed equally

*Correspondence: ximian@sysucc.org.cn (M.X.); zhuyuj@sysucc.org.cn (Y.Z.); liqq@sysucc.org.cn (Q.L.)

Received: June 3, 2026; Accepted: August 26, 2026; Published Online: September 10, 2026; https://doi.org/10.59717/j.xinn-oncol.2026.100040

Citation: Gao Y., Cheng X., Chen B., et al. (2026). Exhaled volatile organic compounds as predictors of chemoradiotherapy response in locally advanced ESCC: A prospective study. *The Innovation Oncology* **1**:100040.

Definitive or neoadjuvant chemoradiotherapy (CRT) is a standard treatment for locally advanced esophageal squamous cell carcinoma (ESCC). However, noninvasive biomarkers for treatment response assessment remain lacking. We investigated the predictive value of exhaled volatile organic compounds (VOCs) in ESCC patients undergoing CRT. In this prospective observational study, exhaled VOCs were analyzed using high-pressure photon ionization time-of-flight mass spectrometry before, during, and after CRT. Patients were classified as complete responders (CR) or non-complete responders (non-CR) based on pathological or imaging assessment. VOCs were selected through univariate analysis, least absolute shrinkage and selection operator regression, and recursive feature elimination. Machine learning models integrating VOCs and clinical variables were developed. Survival outcomes were evaluated using Cox regression and Kaplan–Meier analysis. Among 72 patients enrolled between Oct 8, 2022, and Aug 23, 2023, 44 achieved CR and 28 were classified as non-CR after CRT. Four VOCs and three clinical characteristics were identified as response predictors. Among four machine learning algorithms, the random forest model showed the best performance (AUC, 0.873; sensitivity, 90.9%; specificity, 60.7%; accuracy, 79.2%). The multivariable Cox model predicted 12-month overall survival with an AUC of 0.945. Exhaled VOC profiling represents a promising noninvasive approach for predicting treatment response and survival in ESCC patients receiving CRT.

INTRODUCTION

Esophageal cancer is the 11th most prevalent malignancy worldwide and the 7th leading cause of cancer-related mortality.[1] China represents a high-incidence region, with esophageal squamous cell carcinoma (ESCC) being the predominant histological subtype.[2] The current standard of care for locally advanced ESCC consists of definitive chemoradiotherapy (CRT) or neoadjuvant CRT followed by surgery.[3] However, the identification of reliable biomarkers to predict treatment response after CRT in ESCC remains an unmet clinical need. Although various serum-based biomarkers have been investigated, their performance has been inconsistent and insufficient for clinical utility.[4] For example, circulating tumor DNA (ctDNA) has emerged as a promising liquid biopsy biomarker for predicting therapeutic response and prognosis in several malignancies, including ESCC.[5,6] Nevertheless, its widespread clinical implementation has been hindered by several limitations, such as the lack of standardized detection protocols, vulnerability to pre-analytical variability, and high costs.[7] These challenges underscore the urgent need for developing accurate, noninvasive, and cost-effective biomarkers for assessing treatment response in ESCC.

Human exhaled breath comprises thousands of volatile organic compounds (VOCs), some of which represent metabolic byproducts that enter the lungs via the bloodstream and are subsequently eliminated through gas exchange.[8,9] The VOC profile varies under different physiological and pathological conditions, enabling disease characterization and treatment guidance through precise analytical detection.[10] Substantial evidence has demonstrated the utility of VOCs in cancer diagnosis, therapeutic response prediction, and recurrence monitoring; however, their application in evaluating ESCC treatment efficacy remains unexplored.[11-15]

Gas chromatography–mass spectrometry is the most commonly used analytical technique for VOC detection.[16] However, its clinical implementation is limited by labor-intensive sample preparation, high costs, and requirements for thermal stability.[17] High-pressure photon ionization time-of-flight mass spectrometry (HPPI-TOFMS) provides several advantages, including pretreatment-free operation, cost-effectiveness, resistance to humidity, and enhanced sensitivity, making it a promising alternative for breath analysis.[18] Previous studies have demonstrated the potential of HPPI-TOFMS for cancer detection; however, its utility in predicting treatment efficacy following CRT in ESCC remains unclear.[19-21] This prospective study aimed to longitudinally monitor dynamic changes in VOCs during CRT and evaluate their predictive value for therapeutic efficacy in locally advanced ESCC.

MATERIALS AND METHODS

Study design

The overall study design is presented in Figure 1. Briefly, exhaled breath samples were collected before, during, and after CRT from patients with locally advanced ESCC who received neoadjuvant or definitive CRT in this prospective observational study between October 8, 2022, and August 23, 2023, at Sun Yat-sen University Cancer Center. Patients were stratified into complete response (CR) and non-CR groups based on pathological or imaging assessments and differences in VOC profiles between the two groups were investigated. The study was approved by the Ethics Committee of Sun Yat-sen University Cancer Center and registered at ClinicalTrials.gov (NCT05557955). Written informed consent was obtained from all patients prior to the study procedures.

Participants

Patients 1) aged ≥18 years, 2) with pathologically confirmed ESCC prior to treatment, 3) who had not previously received anticancer therapy, 4) who had stage II–IVA or stage IVB disease with non-regional lymph node metastasis ESCC according to the 8th TNM staging system of the American Joint Committee on Cancer, 5) who were scheduled to undergo neoadjuvant CRT followed by surgery or definitive CRT, 6) who provided written informed consent were included in the analysis.

Conversely, patients who 1) were pregnant or breastfeeding at the time of the study; 2) had a history of malignancies other than esophageal cancer; 3) previously received antitumor therapy, 4) had stage IVB disease and distant metastasis to solid organs; 5) developed conditions rendering patients unfit for CRT (e.g., severe cardiac, pulmonary, hepatic, or renal dysfunction; hematopoietic system disorders; or cachexia); 6) were unable to provide a 0.5-L exhaled breath sample in a single session due to poor physical condition; 7) were unable to provide informed consent because of psychological, familial, or social factors; and 8) had any unstable condition that could compromise patient safety or study compliance were excluded.

Treatment

All patients received concurrent taxane- and platinum-based chemotherapy during radiotherapy, and a subset of patients underwent two cycles of induction chemotherapy prior to definitive CRT. External-beam irradiation was delivered using intensity-modulated radiotherapy. The prescribed dose for definitive CRT was 50–50.4 Gy in 25–28 fractions, whereas 40–45 Gy in 20 fractions was typically administered for neoadjuvant CRT. Esophagectomy

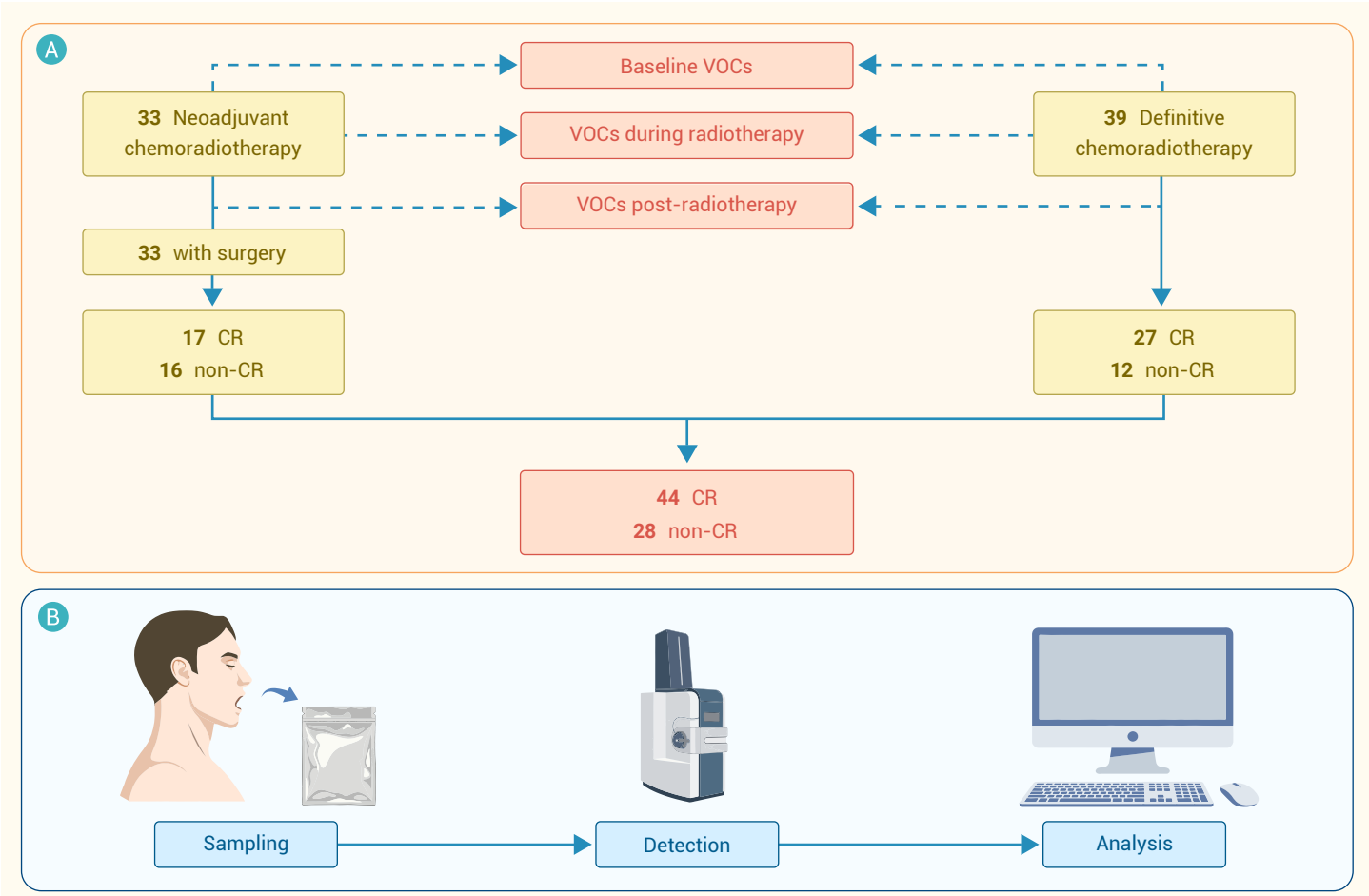

Figure 1. Patient recruitment and sample collection procedures (A) The flow chart depicts the process of patient recruitment and allocation. (B) The workflow illustrates the collection and analysis of exhaled breath samples. VOCs: volatile organic compounds; CR: complete response.

was performed 6–8 weeks after the completion of neoadjuvant CRT. For patients who underwent surgery, CR was defined as the complete absence of residual cancer cells in all layers of the esophagus and in resected lymph nodes. For patients who received definitive CRT, CR was evaluated by computed tomography (CT) or positron emission tomography-CT imaging in combination with endoscopy and biopsy at 3–4 months after CRT completion.[5]

Breath collection

Prior to exhaled breath collection, sampling bags were baked at 60 °C for 3 hours to thoroughly eliminate potential contaminants and subsequently purged four consecutive times with high-purity nitrogen. Exhaled breath samples were collected at baseline, on the day of mid-course radiotherapy, and on the day of completion of radiotherapy. The mid-course breath samples were collected after completion of half of the total prescribed radiotherapy fractions. Trained researchers followed a standardized protocol to ensure consistency. All patients rinsed their mouths with pure water 2 hours prior to sample collection and abstained from food, alcohol, and smoking. The use of toothpaste or mouthwash was prohibited within 15 minutes prior to sampling. After resting in a seated position for 5 minutes in the sampling room, the patients rinsed their mouths with 20 mL of pure water for 10 seconds immediately prior to sampling. Ambient air in the collection chamber was sampled beforehand to minimize environmental interference. Exhaled breath samples were collected using pre-prepared air bags, which were promptly transported to the laboratory and analyzed using HPPI-TOFMS within 4 hours of collection.

HPPI-TOFMS analysis

The structure and working principles of HPPI-TOFMS have been described in detail previously.[18] In brief, the system consists of 1) a high-pressure photon ionization ion source, 2) an ion transmission system, and 3) an orthogonal acceleration TOF mass analyzer. The system operates through dual ionization mechanisms, in which 10.6 eV photons directly ionize compounds with ionization potentials below this threshold to generate molecular ions (M^+), while also facilitating photo-induced chemical ionization processes. The resulting ions are efficiently guided through the system by optimized electric field gradients (16 V→12 V) and focused by a radio frequency-only quadrupole before undergoing pulsed orthogonal acceleration at 33 kHz into the TOF analyzer. Their mass-to-charge ratios are then determined through precise TOF measurements using a 100 ps time-to-digital converter.

Breath data analysis

Given the wide variety of VOCs in exhaled breath, an initial screening of the detected VOCs was performed based on the following criteria: 1) a mean peak intensity greater than 5 and 2) a non-zero peak intensity in more than 90% of the samples. Based on these criteria, 108, 114, and 113 VOCs were identified before, during, and after radiotherapy, respectively. The intersection of these three sets yielded 107 VOCs, which were subsequently subjected to univariate logistic regression. Given the limited sample size, a more liberal threshold ($P < 0.1$) was adopted for univariate screening to reduce the risk of prematurely excluding potentially informative variables. Nineteen VOCs with a P value <0.1 were selected. These VOCs were subsequently subjected to three complementary feature selection methods: LASSO, RF-RFE, and SVM-RFE. LASSO retained nine features corresponding to the minimum cross-validation error. RF-RFE selected four features that achieved the highest prediction accuracy, whereas SVM-RFE retained eight features corresponding to the lowest cross-validation classification error. In addition, three clinical variables with a P value <0.1 in univariate logistic regression were incorporated into the model.

Table 1. VOCs with a *P* value <0.1 in the univariate logistic regression and selected by feature selection methods.

Variable	*P* value	Lasso	RF-RFE	SVM-RFE
m/z=42 (baseline)	0.064		√	√
m/z=43 (baseline)	0.067			
m/z=47 (baseline)	0.089	√		
m/z=54 (baseline)	0.052	√	√	√
m/z=56 (baseline)	0.025	√	√	√
m/z=76 (baseline)	0.080			
m/z=77 (baseline)	0.061			
m/z=85 (baseline)	0.092	√		
m/z=97 (baseline)	0.038	√	√	√
m/z=105 (baseline)	0.050			
m/z=107 (baseline)	0.089			
m/z=108 (baseline)	0.080			
m/z=126 (baseline)	0.058			
m/z=133 (baseline)	0.087			
m/z=28 (during radiotherapy)	0.092	√		
m/z=29 (post-radiotherapy)	0.063	√		√
m/z=43 (post-radiotherapy)	0.068	√		√
m/z=44 (post-radiotherapy)	0.096			
m/z=104 (post-radiotherapy)	0.071	√	√	√

VOCs: volatile organic compounds; RF-RFE: random forest-recursive feature elimination; SVM-RFE: support vector machine- recursive feature elimination.
√: Feature selected by the model.

Model construction

Four machine learning (ML) models—random forest (RF), support vector machine (SVM), K-nearest neighbors (KNN), and eXtreme gradient boosting (XGBoost)—were applied. Owing to the limited sample size, leave-one-out cross-validation was used for internal validation. In each iteration, one patient was held out as the test sample while the remaining patients were used for model training. This process was repeated until every patient had served once as the test sample. Diagnostic performance was optimized using a grid search algorithm to reduce the risk of overfitting. A prognostic model was subsequently developed through multivariate Cox regression analysis based on the selected features. A risk score for each patient was derived from the multivariate Cox analysis. To achieve optimal discrimination, the surv_cutpoint function from the R package survminer was applied, yielding an optimal cutoff value of 2.98. Patients were subsequently stratified into low-risk (risk score <2.98) and high-risk (risk score ≥2.98) groups.

Statistical analysis

Baseline patient characteristics were summarized using descriptive statistics. Changes in VOC peak intensity across the three timepoints were assessed using the Friedman test with pairwise comparisons performed using the Dunn–Bonferroni post-hoc test. Between-group differences in VOC peak intensity were evaluated using the Mann–Whitney U test. VOCs with a *P* value <0.1 in univariate logistic regression were further screened using Lasso, SVM-RFE, and RF-RFE, with the final set of VOCs for model construction determined based on the intersection of these three methods (Table 1). The performance of ML models was evaluated in terms of sensitivity, specificity, accuracy, area under the curve (AUC), and decision curve analysis (DCA). The optimal model was selected based on the AUC. SHAP values were calculated for each feature using the optimal model. Overall survival (OS) was defined as the interval from enrollment to death from any cause or last follow-up. A multivariate Cox analysis was used to construct a prognostic model based on the selected features. Model accuracy was further evaluated using time-dependent receiver operating characteristic (ROC) curves. Survival analyses were performed using Kaplan–Meier estimates with comparisons assessed by the log-rank test. All statistical analyses and model construction were performed using RStudio 4.3.2. SHAP value analyses were conducted using Python version 3.9. A *P* value <0.05 was considered significant.

RESULTS

Patient characteristics

In total, 72 patients with ESCC were included in this study. The median age was 61 years, and the majority of the participants were men (75.0%). Of these, 39 patients received definitive CRT, whereas 33 underwent neoadjuvant CRT followed by surgery. CR was achieved in 44 patients, whereas non-CR was observed in 28 patients after CRT. The recruitment process and clinical characteristics are presented in Figure 1A and Table 2. Additionally, a schematic illustration of the sample collection and detection process is provided in Figure 1B. At the data cutoff date of January 15, 2025, the median follow-up duration was 20.9 months (interquartile range: 17.1–23.2), and the 1-year OS for the entire cohort was 87.5%.

Prediction model construction based on breath test

Four VOCs—m/z=54 (baseline), m/z=56 (baseline), m/z=97 (baseline), and m/z=104 (post-radiotherapy)—together with three clinical characteristics (tumor length, tumor location, and T stage) were incorporated into model development (Table 3). Based on these variables, four ML models were constructed to predict CR in patients with ESCC after CRT. Figure 2 presents the ROC curves of the four models, with their discriminative performance quantified by the AUC. The RF model achieved the highest AUC (0.873, 95%CI 0.794-0.953), followed by XGBoost (0.703, 95%CI 0.578-0.828), SVM (0.672, 95%CI 0.539-0.805), and KNN (0.626, 95%CI 0.5-0.752). Clinical applicability was further evaluated using DCA (Figure S1). The RF model provided consistently superior net benefit compared with the baseline across threshold probabilities of 0.2–0.85, whereas XGBoost showed optimal performance within

Table 2. Patients' baseline clinical characteristics.

Characteristic	Total (n=72), %	CR (n=44), %	non-CR (n=28), %
Age (years)			
Median (range)	61 (38–79)	60 (38–79)	64 (40–74)
Sex			
Male	54 (75.0)	31 (70.4)	23 (82.1)
Female	18 (25.0)	13 (29.6)	5 (17.9)
Smoking history			
Yes	38 (52.8)	22 (50.0)	16 (57.1)
No	34 (47.2)	22 (50.0)	12 (42.9)
Alcohol history			
Yes	35 (48.6)	19 (43.2)	16 (57.1)
No	37 (51.4)	25 (56.8)	12 (42.9)
BMI (kg/m^2)			
<18.5	6 (8.3)	4 (9.1)	2 (7.1)
≥18.5	66 (91.7)	40 (90.9)	26 (92.9)
Histologic grade			
Gx/1/2	47 (65.3)	30 (68.2)	17 (60.7)
G3	25 (34.7)	14 (31.8)	11 (39.3)
Tumor location			
Upper	20 (27.8)	17 (38.6)	3 (10.7)
Middle thoracic	22 (30.5)	11 (25.0)	11 (39.3)
Distal thoracic	30 (41.7)	16 (36.4)	14 (50.0)
Primary tumor length			
<5 cm	27 (37.5)	21 (47.7)	6 (21.4)
≥5 cm	45 (62.5)	23 (52.3)	22 (78.6)
Clinical TNM stage			
II	8 (11.1)	8 (18.2)	0 (0.0)
III	36 (50.0)	19 (43.2)	17 (60.7)
IV	28 (38.9)	17 (38.6)	11 (39.3)
T stage			
1–2	22 (30.6)	18 (40.9)	4 (14.3)
3–4	50 (69.4)	26 (59.1)	24 (85.7)
N stage			
0–2	58 (80.6)	37 (84.1)	21 (75.0)
3	14 (19.4)	7 (15.9)	7 (25.0)
M stage			
0	64 (88.9)	40 (90.9)	24 (85.7)
1	8 (11.1)	4 (9.1)	4 (14.3)
Treatment patterns			
Definitive chemoradiotherapy	39 (54.2)	27 (61.4)	12 (42.9)
Neoadjuvant chemoradiotherapy	33 (45.8)	17 (38.6)	16 (57.1)

CR: complete response; BMI: body mass index.

Table 3. Variables incorporated into the predictive models.

Variable	Odds ratio (95%CI)	*P* value
m/z=54 (baseline)	1.008 (1.000–1.016)	0.058
m/z=56 (baseline)	1.060 (1.012–1.121)	0.025
m/z=97 (baseline)	0.995 (0.990–0.999)	0.038
m/z=104 (post-radiotherapy)	0.971 (0.936–0.997)	0.071
T stage (T1–2 vs. T3–4)	0.241 (0.063–0.754)	0.022
Tumor location (upper vs. middle/lower)	0.191 (0.041–0.652)	0.016
Tumor length (<5 vs. ≥5 cm)	0.299 (0.095–0.843)	0.028

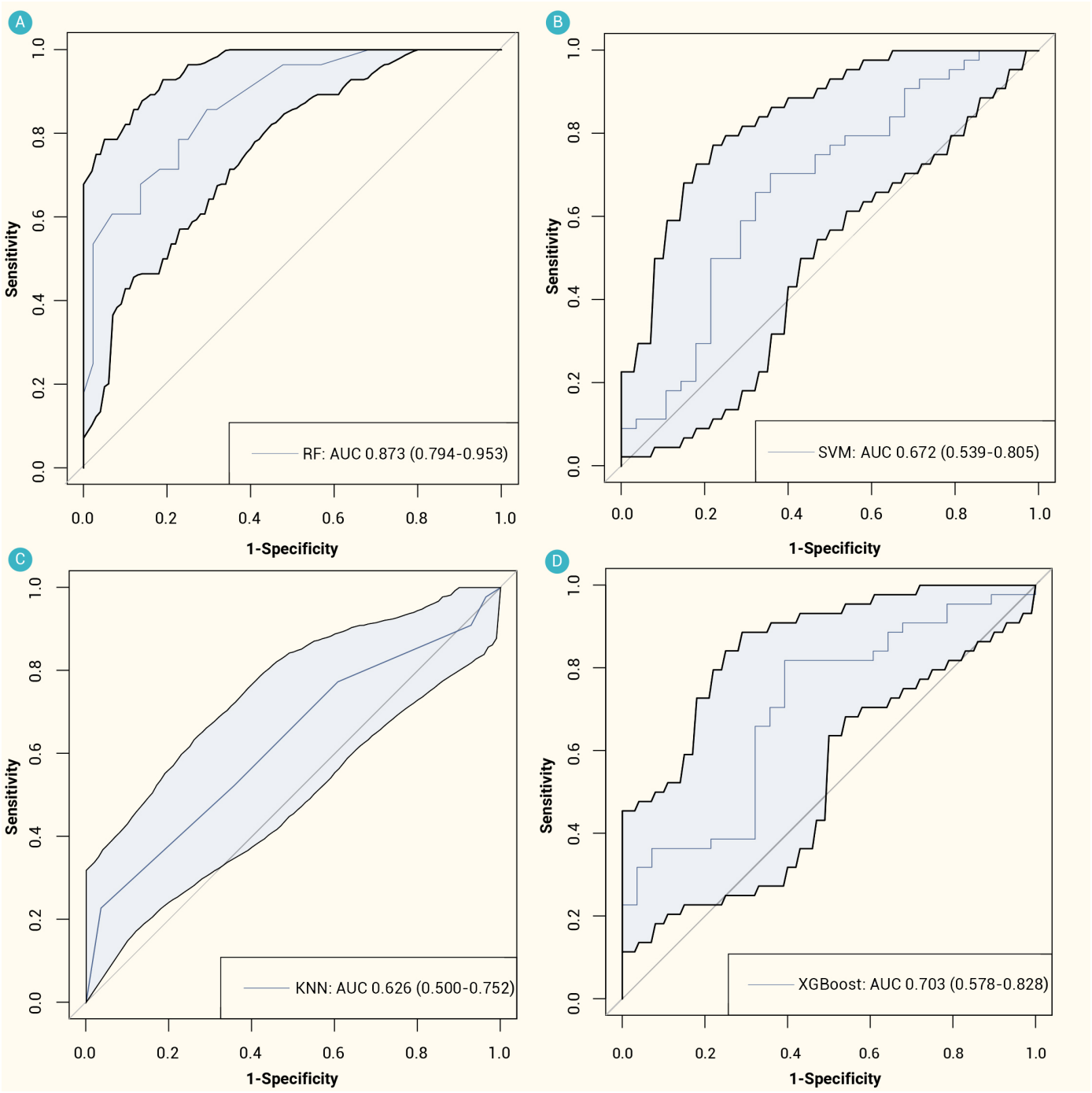

Figure 2. Receiver operating characteristic curves of machine learning models for predicting CR (A) ROC curve for RF. (B) ROC curve for SVM. (C) ROC curve for KNN. (D) ROC curve for XGBoost. CR: complete response; RF: random forest; AUC: area under curve; KNN: K-nearest neighbor; ROC: receiver operating characteristic; SVM: support vector machine; XGBoost: eXtreme gradient boosting.

Table 4. Sensitivity, specificity, and accuracy of the machine learning models for predicting CR in patients with ESCC.

Model	Sensitivity	Specificity	Accuracy
RF	90.9%	60.7%	79.2%
SVM	67.3%	58.8%	65.3%
KNN	39.3%	77.3%	62.5%
XGBoost	60.7%	72.7%	68.1%

CR: complete response; RF: random forest; SVM: support vector machine; KNN: k-nearest neighbor; XGBoost: eXtreme gradient boostingta.

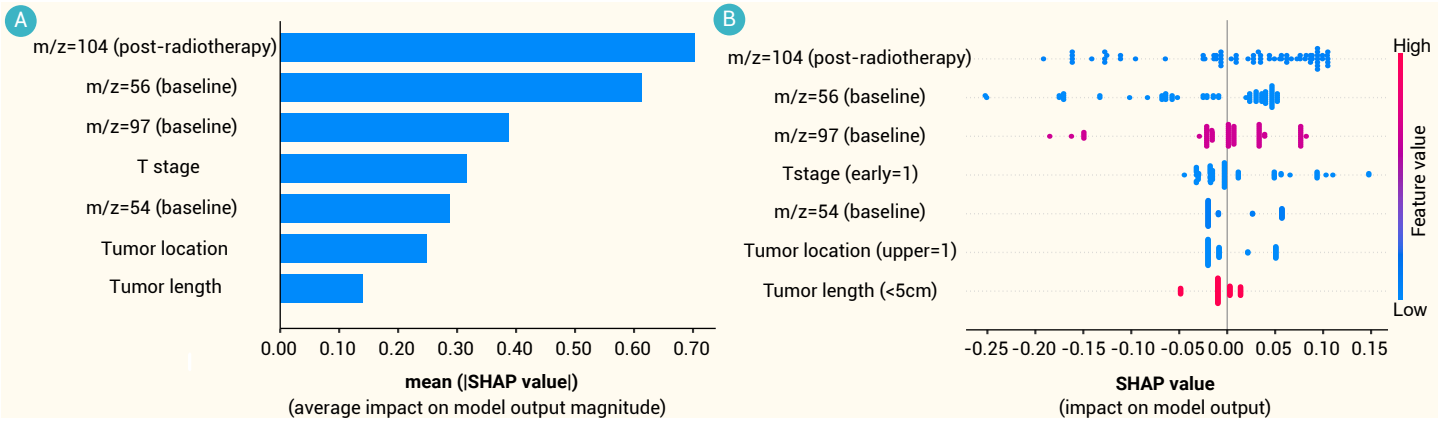

Figure 3. Feature-ranking plots (A) and beeswarm plots (B) of the random forest model for predicting CR The color indicates the feature value, while the SHAP value on the x-axis represents the contribution of that feature to the model prediction. Patients with the same feature value may exhibit different SHAP values due to interactions among features and the non-linear nature of the model. RF: random forest; CR: complete response.

the 0.4–0.7 threshold range. By contrast, both SVM and KNN models yielded relatively lower net benefits. Additionally, the accuracy, sensitivity, and specificity were calculated for all four models (Table 4). The RF model demonstrated the highest accuracy (79.2%) and sensitivity (90.9%). Although its specificity was not the highest, the RF model exhibited the best overall performance when these metrics were considered comprehensively.

To elucidate how individual features contributed to the predictive performance of the RF model, the SHAP value of each variable was calculated. As illustrated in Figure 3A, features were ranked according to their relative contribution to CR prediction. The most influential feature was m/z=104 (post-radiotherapy), followed by m/z=56 (baseline), m/z=97 (baseline), T stage, m/z=54 (baseline), tumor location, and tumor length. Figure 3B further depicts the associations between feature values and CR probability. Specifically, early T stage, upper tumor location, shorter tumor length, lower levels of m/z=104 (post-radiotherapy) and m/z=97 (baseline), and higher levels of m/z=56 (baseline) and m/z=54 (baseline) were associated with a higher likelihood of achieving CR.

Furthermore, dynamic changes in the four VOCs were evaluated during treatment, revealing varying degrees of alteration in peak intensities as therapy progressed (Figure S2). Comparative analysis between the CR and non-CR groups demonstrated that patients with CR consistently exhibited higher peak intensities of m/z=54 and m/z=56 before and after treatment, whereas patients in the non-CR group showed higher peak intensities of m/z=97 and m/z=104 (Figure S3).

Prognostic model construction based on breath test

The prognostic value of VOCs and clinical features for OS was evaluated using multivariate Cox analysis (Figure 4A). None of these features emerged as independent prognostic factors. However, based on the multivariate regression model, a risk score was calculated for each patient, and the patients were stratified into low-risk and high-risk groups according to the optimal cutoff value (2.98). The ROC curve of the prognostic model yielded an AUC value of 0.945 (95%CI: 0.89-1.00) for predicting the 12-month OS (Figure 4B). The KM survival analysis indicated a significant difference (P<0.05) in OS between the high- and low-risk groups (Figure 4C).

DISCUSSION

In this prospective observational study, HPPI-TOFMS was employed to analyze breath omics profiles before, during, and after radiotherapy, with the aim of identifying predictive breath biomarkers in patients with ESCC treated with CRT. A panel of four VOCs, in combination with three clinical variables, effectively distinguished between patients with CR and non-CR and demonstrated promising predictive value for OS.

Several studies have explored the role of VOCs in cancer diagnosis and treatment efficacy. One study demonstrated the feasibility of predicting short-term efficacy in patients with ESCC receiving neoadjuvant chemoimmunotherapy using VOCs.[22] Similarly, De Vries et al. reported that baseline VOCs could predict the efficacy of anti-programmed cell death protein 1 antibodies in patients with non-small cell lung cancer.[23] However, these investigations were limited to the analysis of VOC levels exclusively at the pre-treatment stage. Reliance on pre-treatment VOC measurements alone neglects the impact of treatment on tumor metabolism and the tumor microenvironment. In a separate study, Wang et al. explored perioperative VOC dynamics in patients with lung cancer and observed significant post-treatment alterations in the levels of specific VOC classes, including aldehydes, hydrocarbons, and ketones.[19] Similarly, the present study evaluated the levels of four VOCs incorporated into the predictive model before, during, and after treatment. Significant differences in VOC levels were observed throughout the treatment course. This finding further indicates that dynamic monitoring of VOCs during treatment provides a more comprehensive assessment of tumor metabolic status, as it captures real-time changes in tumor biology that static pre-treatment measurements alone cannot reveal.

Furthermore, most previous studies developed models based solely on VOCs. By contrast, the present model incorporated both VOCs and clinical features as predictive variables. Models relying exclusively on VOCs are vulnerable to interference from non-pathological factors, which may reduce their generalizability across patient populations. The integration of clinical features facilitated multi-dimensional patient profiling, thereby enhancing model robustness and enabling the identification of potential target groups. Although the AUC of our predictive model did not demonstrate a significant advantage over those reported in the previous studies, a more comprehensive modeling framework was employed. The incorporation of dynamic VOC

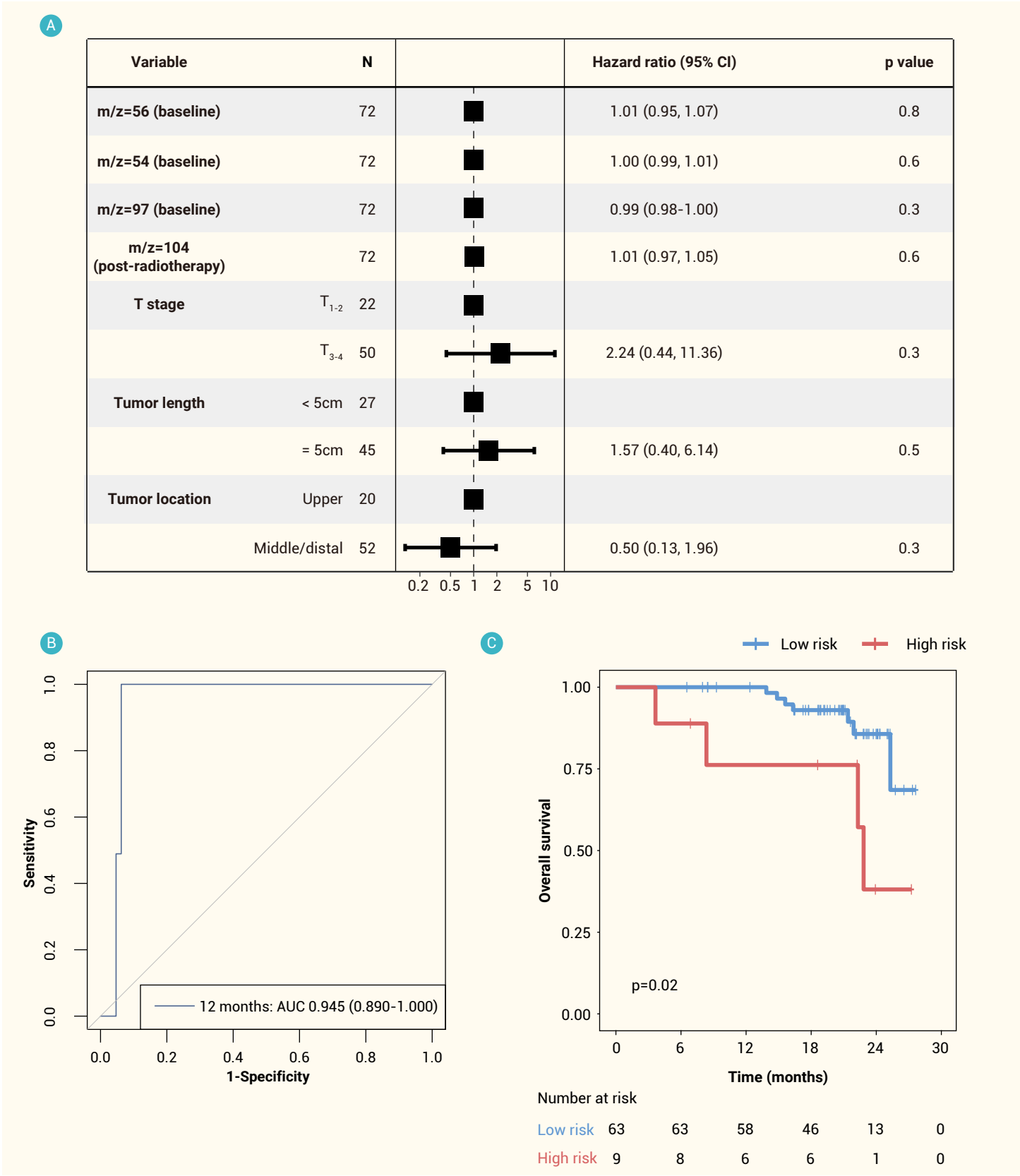

Figure 4. Prognostic model for overall survival constructed using the variables selected in the RF model (A) Forest plot presenting the multivariate Cox regression analysis for overall survival. (B) ROC curve evaluating the predictive performance for 12-month overall survival. (C) Kaplan–Meier analysis for overall survival between the high-risk and low-risk groups. ROC: receiver operating characteristic. Squares represent ORs, and horizontal lines represent 95% CIs. The vertical dashed line indicates OR = 1.

data with clinical features enabled a holistic assessment of patients, addressing the limitations of static or single-variable models. This approach is consistent with previous research: Liu et al. incorporated clinical risk factors into a breast cancer diagnostic model, demonstrating that the combination of VOCs with clinical features yielded superior predictive performance compared with VOC-only models.[20] In summary, compared with previous studies, our research investigated longitudinal changes in VOC levels in patients with locally advanced ESCC before and after CRT. By integrating

clinical characteristics, both the predictive value of VOCs for short-term efficacy and their role in survival prediction were explored. Ultimately, VOC-based prediction models demonstrated substantial potential for predicting tumor response and OS.

The biological mechanisms underlying VOC alterations remain incompletely understood. Previous studies suggest that tumor-associated oxidative stress, hypoxia, metabolic reprogramming, and genetic alterations may all contribute to changes in endogenous VOC production.[9,24] During radiotherapy, ionizing radiation exerts direct cytotoxic effects, inducing cell death. Concurrently, interactions between radiation and surrounding water molecules trigger the ionization of a large number of water molecules, resulting in the formation of hydroxyl radicals.[25] These hydroxyl radicals not only exacerbate cell death but also cause damage to other macromolecules, thereby contributing to the increased production of VOCs. Therefore, the VOC changes observed during treatment likely reflect a combination of tumor biology and treatment-induced metabolic responses.

The results obtained from HPPI-TOFMS characterized specific VOCs by their m/z values but did not allow for precise structural identification. Using the Human Breathomics Database,[26] m/z values of 54 and 56 were tentatively assigned to butadiene and butene, whereas m/z = 97 may represent a fatty acid cleavage fragment associated with lipid peroxidation. Given that chemoradiotherapy induces oxidative stress, changes in these VOCs may reflect both treatment-related metabolic alterations and tumor-associated biological processes. The m/z = 104 signal was preliminarily assigned to styrene, which has previously been reported as a candidate exhaled biomarker in lung cancer.[19] In our cohort, m/z = 104 showed the highest baseline abundance and progressively decreased during treatment while remaining consistently higher in non-CR patients, suggesting a potential association with tumor burden and treatment response. Nevertheless, these compound assignments remain tentative and require confirmation using complementary analytical platforms.

From a clinical perspective, early prediction of treatment response is crucial for optimizing the management of locally advanced ESCC, as radiological changes often lag behind biological responses. Dynamic breath VOC monitoring may detect treatment-related metabolic changes earlier than conventional imaging and serve as a complementary, noninvasive, rapid, and repeatable approach for serial assessment during CRT. Such information may facilitate timely treatment adaptation and support individualized therapeutic decision-making.

This study has several limitations. The single-center design, relatively small sample size, and lack of external validation may limit the robustness and generalizability of the model. In addition, HPPI-TOFMS provides only mass-to-charge ratios rather than definitive chemical identities, requiring further analytical validation. The inclusion of both cCR and pCR may also introduce response heterogeneity. Furthermore, post-treatment breath samples were collected immediately after radiotherapy, when radiation-induced inflammation may influence VOC profiles. Future multicenter studies with larger cohorts, longitudinal follow-up, external validation, and stratified analyses of different response categories are warranted.

CONCLUSION

In conclusion, this study proposes a novel, noninvasive VOC-based approach for predicting treatment response in patients with ESCC treated with CRT. These findings underscore the potential of exhaled breath analysis to serve as a complementary tool in the clinical management of ESCC.

REFERENCES

1. Bray F., Laversanne M., Sung H., et al. (2024). Global cancer statistics 2022: GLOBOCAN estimates of incidence and mortality worldwide for 36 cancers in 185 countries. *CA Cancer J. Clin.* **74**:229–263. DOI:10.3322/caac.21834
2. Kamangar F., Nasrollahzadeh D., Safiri S., et al. (2020). The global, regional, and national burden of oesophageal cancer and its attributable risk factors in 195 countries and territories, 1990–2017: A systematic analysis for the Global Burden of Disease Study 2017. *Lancet Gastroenterol.* **5**:582–597. DOI:10.1016/S2468-1253(20)30007-8
3. Yang H., Wang F., Hallemeier C.L., et al. (2024). Oesophageal cancer. *Lancet* **404**:1991–2005. DOI:10.1016/s0140-6736(24)02226-8
4. Chu L.Y., Peng Y.H., Weng X.F., et al. (2020). Blood-based biomarkers for early detection of esophageal squamous cell carcinoma. *World J. Gastroenterol.* **26**:1708–1725. DOI:10.3748/wjg.v26.i15.1708
5. Chen B., Liu S., Zhu Y., et al. (2024). Predictive role of ctDNA in esophageal squamous cell carcinoma receiving definitive chemoradiotherapy combined with toripalimab. *Nat. Commun.* **15**:1919. DOI:10.1038/s41467-024-46307-7
6. Pan Y., Zhang J.T., Gao X., et al. (2023). Dynamic circulating tumor DNA during chemoradiotherapy predicts clinical outcomes for locally advanced non-small cell lung cancer patients. *Cancer Cell* **41**:1763–1773.e1764. DOI:10.1016/j.ccell.2023.09.007
7. Farshchi F. and Hasanzadeh M. (2023). Efficient diagnosis of cancer using biosensing of circulating tumor DNAs(ctDNA): Recent progress and challenges. *Biomed. Pharmacother.* **193**:109076. DOI:https://doi.org/10.1016/j.microc.2023.109076
8. Drabińska N., Flynn C., Ratcliffe N., et al. (2021). A literature survey of all volatiles from healthy human breath and bodily fluids: The human volatilome. *J. Breath Res.* **15**. DOI:10.1088/1752-7163/abf1d0
9. Haick H., Broza Y.Y., Mochalski P., et al. (2014). Assessment, origin, and implementation of breath volatile cancer markers. *Chem. Soc. Rev.* **43**:1423–1449. DOI:10.1039/c3cs60329f
10. Binson V.A. and Subramoniam M. (2022). Exhaled breath volatile organic compound analysis for the detection of lung cancer- a systematic review. *Journal of Biomimetics, Biomaterials and Biomedical Engineering* **56**:17–35. DOI:10.4028/p-dab04j
11. Nardi-Agmon I., Abud-Hawa M., Liran O., et al. (2016). Exhaled breath analysis for monitoring response to treatment in advanced lung cancer. *J. Thorac. Oncol.* **11**:827–837. DOI:10.1016/j.jtho.2016.02.017
12. Sukaram T., Apiparakoon T., Tiyarattanachai T., et al. (2023). VOCs from exhaled breath for the diagnosis of hepatocellular carcinoma. *Diagnostics* **13**:257. DOI:10.3390/diagnostics13020257
13. Liu Y., Ji Y., Chen J., et al. (2024). Pioneering noninvasive colorectal cancer detection with an AI-enhanced breath volatilomics platform. *Theranostics* **14**:4240–4255. DOI:10.7150/thno.94950
14. Kumar S., Huang J., Abbassi-Ghadi N., et al. (2015). Mass spectrometric analysis of exhaled breath for the identification of volatile organic compound biomarkers in esophageal and gastric adenocarcinoma. *Ann. Surg.* **262**:981–990. DOI:10.1097/sla.0000000000001101
15. Hanevelt J., Schoenaker I.J.H., Brohet R.M., et al. (2023). Alteration of the exhaled volatile organic compound pattern in colorectal cancer patients after intentional curative surgery-a prospective pilot study. *Cancers (Basel)* **15**:4785. DOI:10.3390/cancers15194785
16. Davis M.D., Fowler S.J. and Montpetit A.J. (2019). Exhaled breath testing - a tool for the clinician and researcher. *Paediatr. Respir. Rev.* **29**:37–41. DOI:10.1016/j.prrv.2018.05.002
17. Lubes G. and Goodarzi M. (2018). GC-MS based metabolomics used for the identification of cancer volatile organic compounds as biomarkers. *J. Pharm. Biomed. Anal.* **147**:313–322. DOI:10.1016/j.jpba.2017.07.013
18. Wang Y., Jiang J., Hua L., et al. (2016). High-pressure photon ionization source for TOFMS and its application for online breath analysis. *Anal. Chem.* **88**:9047–9055. DOI:10.1021/acs.analchem.6b01707
19. Wang P., Huang Q., Meng S., et al. (2022). Identification of lung cancer breath biomarkers based on perioperative breathomics testing: A prospective observational study. *EClinicalMedicine* **47**:101384. DOI:10.1016/j.eclinm.2022.101384
20. Liu J., Chen H., Li Y., et al. (2023). A novel non-invasive exhaled breath biopsy for the diagnosis and screening of breast cancer. *J. Hematol. Oncol.* **16**:63. DOI:10.1186/s13045-023-01459-9
21. Huang Q., Wang S., Li Q., et al. (2021). Assessment of breathomics testing using high-pressure photon ionization time-of-flight mass spectrometry to detect esophageal cancer. *JAMA Netw. Open* **4**:e2127042. DOI:10.1001/jamanetworkopen.2021.27042
22. Huang Q., Liu Z., Yu Y., et al. (2024). Prediction of response to neoadjuvant chemo-immunotherapy in patients with esophageal squamous cell carcinoma by a rapid breath test. *Br. J. Cancer* **130**:694–700. DOI:10.1038/s41416-023-02547-w
23. de Vries R., Muller M., van der Noort V., et al. (2019). Prediction of response to anti-PD-1 therapy in patients with non-small-cell lung cancer by electronic nose analysis of exhaled breath. *Ann. Oncol.* **30**:1660–1666. DOI:10.1093/annonc/mdz279
24. Hanahan D. (2022). Hallmarks of cancer: New dimensions. *Cancer Discov.* **12**:31–46. DOI:10.1158/2159-8290.Cd-21-1059
25. Petroni G., Cantley L.C., Santambrogio L., et al. (2022). Radiotherapy as a tool to elicit clinically actionable signalling pathways in cancer. *Nat. Rev. Clin. Oncol.* **19**:114–131. DOI:10.1038/s41571-021-00579-w
26. Kuo T.-C., Tan C.-E., Wang S.-Y., et al. (2020). Human breathomics database. *Database-Oxford* **2020**:baz139. DOI:10.1093/database/baz139

FUNDING AND ACKNOWLEDGMENTS

This study was supported by the National Natural Science Foundation of China (82172669, 82373214, 82473241, and 82573436), Guangdong Basic and Applied Basic Research Foundation (2025B1515020090 and 2025A1515010951), and Young Talents Program of Sun Yat-sen University Cancer Center (PT22121101 and PT22121201). The

funders had no role in study design, data collection and analysis, decision to publish, or preparation of the manuscript.

AUTHOR CONTRIBUTIONS

Y. Gao: Data curation, investigation, formal analysis, visualization, writing-original draft, and writing-review editing. X. Cheng: Data curation, investigation, formal analysis, visualization, writing-original draft, and writing-review editing. B. Chen: Data curation, investigation, formal analysis, writing-original draft and writing-review editing. L. Zhao: Data curation, investigation, visualization, and writing-review editing. S. Liu and Y. Lv: Data curation, investigation, and writing-review editing. Q. Li and Y. Zhu: Conceptualization, supervision, and writing-review editing. M. Xi: Conceptualization, data curation, formal analysis, supervision, funding acquisition, visualization, writing-original draft, and writing-review editing. All authors contributed to the manuscript and approved the final version.

DECLARATION OF INTERESTS

The authors declare no competing interests.

ETHICAL STATEMENT AND PATIENT CONSENT

This study has been approved by the Ethic Committee of Sun Yat-sen University Cancer Center (B2022-474-01) and registered at ClinicalTrials.gov (NCT05557955). Written informed consent was obtained from all participants.

DATA AND CODE AVAILABILITY

Research data are stored in an institutional repository (www.researchdata.org.cn) and will be shared upon request to the corresponding author.

SUPPLEMENTAL INFORMATION

It can be found online at https://doi.org/10.59717/j.xinn-oncol.2026.100040